A large bistable negative lens by integrating a polarization switch with a passively anisotropic focusing element

Hung-Shan Chen,[1] Yi-Hsin Lin,[1,*] Abhishek Kumar Srivastava,[2] Vladimir Grigorievich Chigrinov,[2] Chia-Ming Chang,[1] and Yu-Jen Wang[1]

[1]*Department of Photonics, National Chiao Tung University, Hsinchu, Taiwan*
[2]*State Key Lab on Advanced Displays and Optoelectronics, Department of Electronic and Computer Engineering, Hong Kong University of Science and Technology, Hong Kong, China*
[*]*yilin@mail.nctu.edu.tw*
http://web.it.nctu.edu.tw/~yilin/

Abstract: A bistable negative lens with a large aperture size (~10mm) by integrating a polarization switch of ferroelectric liquid crystals (FLCs) with a passively anisotropic focusing element is demonstrated. The proposed lens not only exhibits electrically tunable bistability but also fast response time of sub-milliseconds. The tunable lens power is from 0 to −1.74 Diopters. The electro-optical properties and imaging performances are demonstrated. The impact of this study is to provide a solution of electrically bistable liquid crystal lenses for the applications of portable devices, wearable devices and colored ophthalmic lenses.

OCIS codes: (160.5470) Polymers; (230.3720) Liquid-crystal devices; (230.2090) Electro-optical devices.

References and links

1. S. Sato, "Liquid-crystal lens-cells with variable focal length," Jpn. J. Appl. Phys. **18**(9), 1679–1684 (1979).
2. H. Ren and S. T. Wu, *Introduction to Adaptive Lenses* (John Wiley, 2012).
3. L. W. Li, D. Bryant, T. Van Heugten, and P. J. Bos, "Speed, optical power, and off-axis imaging improvement of refractive liquid crystal lenses," Appl. Opt. **53**(6), 1124–1131 (2014).
4. K. Asatryan, V. Presnyakov, A. Tork, A. Zohrabyan, A. Bagramyan, and T. Galstian, "Optical lens with electrically variable focus using an optically hidden dielectric structure," Opt. Express **18**(13), 13981–13992 (2010).
5. M. Kawamura, M. Ye, and S. Sato, "Optical trapping and manipulation system using liquid-crystal lens with focusing and deflection properties," Jpn. J. Appl. Phys. **44**(8), 6098–6100 (2005).
6. Y. H. Lin and H. S. Chen, "Electrically tunable-focusing and polarizer-free liquid crystal lenses for ophthalmic applications," Opt. Express **21**(8), 9428–9436 (2013).
7. H. C. Lin and Y. H. Lin, "A fast response and large electrically tunable-focusing imaging system based on switching of two modes of a liquid crystal lens," Appl. Phys. Lett. **97**(6), 063505 (2010).
8. H. C. Lin and Y. H. Lin, "An electrically tunable focusing pico-projector adopting a liquid crystal lens," Jpn. J. Appl. Phys. **49**(10), 102502 (2010).
9. Y. H. Lin, M. S. Chen, and H. C. Lin, "An electrically tunable optical zoom system using two composite liquid crystal lenses with a large zoom ratio," Opt. Express **19**(5), 4714–4721 (2011).
10. H. C. Lin, N. Collings, M. S. Chen, and Y. H. Lin, "A holographic projection system with an electrically tuning and continuously adjustable optical zoom," Opt. Express **20**(25), 27222–27229 (2012).
11. Y. S. Tsou, Y. H. Lin, and A. C. Wei, "Concentrating photovoltaic system using a liquid crystal lens," IEEE Photon. Technol. Lett. **24**(24), 2239–2242 (2012).
12. H. S. Chen and Y. H. Lin, "An endoscopic system adopting a liquid crystal lens with an electrically tunable depth-of-field," Opt. Express **21**(15), 18079–18088 (2013).
13. G. Li, P. Valley, P. Äyräs, D. L. Mathine, S. Honkanen, and N. Peyghambarian, "High-efficiency switchable flat diffractive ophthalmic lens with three-layer electrode pattern and two-layer via structures," Appl. Phys. Lett. **90**(11), 111105 (2007).
14. H. C. Lin, M. S. Chen, and Y. H. Lin, "A review of electrically tunable focusing liquid crystal lenses," Trans. Electr. Electron Mater. **12**(6), 234–240 (2011).
15. M. Ye, B. Wang, M. Uchida, S. Yanase, S. Takahashi, M. Yamaguchi, and S. Sato, "Low-voltage-driving liquid crystal lens," Jpn. J. Appl. Phys. **49**(10), 100204 (2010).
16. H. C. Lin and Y. H. Lin, "An electrically tunable-focusing liquid crystal lens with a low voltage and simple electrodes," Opt. Express **20**(3), 2045–2052 (2012).

#209037 - $15.00 USD Received 27 Mar 2014; revised 7 May 2014; accepted 16 May 2014; published 22 May 2014

17. A. F. Naumov, G. D. Love, M. Y. Loktev, and F. L. Vladimirov, "Control optimization of spherical modal liquid crystal lenses," Opt. Express **4**(9), 344–352 (1999).
18. F. Fan, A. K. Srivastava, T. Du, M. C. Tseng, V. G. Chigrinov, and H. S. Kwok, "Low voltage tunable liquid crystal lens," Opt. Lett. **38**(20), 4116–4119 (2013).
19. X. Q. Wang, A. K. Srivastava, V. G. Chigrinov, and H. S. Kwok, "Switchable Fresnel lens based on micropatterned alignment," Opt. Lett. **38**(11), 1775–1777 (2013).
20. Y. M. Lee, K. H. Lee, Y. Choi, and J. H. Kim, "Fast bistable microlens arrays based on a birefringence layer and ferroelectric liquid crystals," Jpn. J. Appl. Phys. **47**(8), 6343–6346 (2008).
21. S. T. Largerwall, *Ferroelectric and Antiferroelectric Liquid Crystals* (John Wiley, 1999).
22. P. Xu, X. Li, A. Muravski, V. Chigrinov, and S. Valyukh, "Photoaligned bistable FLC displays with birefringent color switching," SID 06 Digest (2006), 854.
23. E. Pozhidaev, V. Chigrinov, and X. Li, "Photoaligned ferroelectric liquid crystal passive matrix display with memorized gray scale," Jpn. J. Appl. Phys. **45**(2A), 875–882 (2006).
24. P. Yeh and C. Gu, *Optics of Liquid Crystal Displays* (John Wiley, 2010).
25. Y. Geng, J. Sun, A. Murauski, V. Chigrinov, and H. S. Kwok, "Increasing the rewriting speed of optical rewritable e-paper by selecting proper liquid crystals," Chin. Phys. B **21**(8), 080701 (2012).
26. P. Hariharan and P. E. Ciddor, "Improved switchable achromatic phase shifters," Opt. Eng. **38**(6), 1078–1080 (1999).
27. Q. Guo, A. K. Srivastava, E. P. Pozhidaev, V. G. Chigrinov, and H. S. Kwok, "Optimization of alignment quality of ferroelectric liquid crystals by controlling anchoring energy," Appl. Phys. Express **7**(2), 021701 (2014).

1. Introduction

Electrically tunable focusing liquid crystal (LC) lenses have many applications in imaging systems and projection systems, such as portable devices, pico projections, optical trapping, endoscopy, solar cells, optical zoom systems, and ophthalmic lenses [1–13]. The optical mechanism of LC lenses is that a wavefront conversion resulting from the spatial distribution of optical path difference owing to a spatial distribution of refractive indices or a spatial distribution of thickness of the LC layer or both of a spatial variations of the refractive indices and thickness of the LC layer [1, 2, 14]. Many researchers proposed different structures to carry out electrically tunable lensing effect by adopting LC materials, such as a LC lens with a hole-patterned electrode and a LC lens with a spatially distributed dielectric layer [15–17]. Another approach exploits the initial guidance of the LC director, by mean of photoalignment, to create a variable distribution of pre-tilt angles of the LC director for obtaining an equivalent lens profile [18, 19]. Recently, we also demonstrated a polarizer-free LC lens with large aperture size (~6mm) for ophthalmic applications using a double-layered structure [6]. However, all of them require constantly application of voltages that means constant power consumption. For ophthalmic applications or many applications, bistability is required. Moreover, the switching speed of LC lenses is slow in general (>500 ms) [7]. S. Sato demonstrated a LC lens with two focal lengths by means of a combination of two LC devices: one is an anisotropic LC lens and the other is a twisted nematic (TN) LC cell functioning as a polarization switch [1]. Nevertheless, the response time of TN LC cell is slow and poor image quality resulting from severe scattering of anisotropic LC lens with a cell gap of 450 μm regardless of large aperture of 20 mm. Y. M. Lee et. al., proposed a bistable LC lens arrays with a positive focal length by means of a LC polymer layer and ferroelectric liquid crystal (FLC) cell [20]. The primary disadvantage is poor image quality because of the non-uniform polarization switch and defects, results of inhomogeneous electric fields applying to FLC layer originating from the thickness variation of the a LC polymer layer. Based on the results of the high driving voltage (± 40V) and small aperture size of a sub-lens~0.2 mm, the driving voltage is at least 800V for realizing the aperture size of a sub-lens of 10 mm. In addition, tunable focusing negative lenses are also important for reduction of aberrations and extension of field-of-view in optical systems, but such negative lenses are still under development. In this paper, we propose a negative lens with large aperture size (~10mm) by ferroelectric liquid crystal (FLC) switch and liquid crystal and polymer composite (LCPC) lens. The proposed lens structure not only exhibits electrically tunable bistability but also fast response time of sub-milliseconds with low driving voltage (~10V). To our knowledge, this is the first time to demonstrate a bistable LC lens with large aperture size (~10mm) and good image quality. This study opens a window for developing bistable LC lenses, which makes lots of

#209037 - $15.00 USD Received 27 Mar 2014; revised 7 May 2014; accepted 16 May 2014; published 22 May 2014

application more practical, such as imaging systems for portable device, wearable devices, and ophthalmic lenses.

2. Operating principle and sample preparation

The structure and operating principles of the bistable negative lens are depicted in Fig. 1(a) and Fig. 1(b). The structure is made up of three parts: a polarizer, a FLC part and a liquid crystal and polymer composite (LCPC) part. The FLC part consists of a FLC layer sandwiched between two ITO glass substrates, where one of the ITO glass substrate is coated with photo-alignment layer. The LCPC part consists of a layer of liquid crystal and polymer composite (LCPC) sandwiched between a curved glass substrate and a flat glass substrate, which are also coated with alignment layers with an anti-parallel configuration. By means of designing the phase retardation of the FLC layer as a half-wave retarder, the function of the FLC part is an active bistable polarization switch for switching between two linear polarization states of incident light: x-linearly polarized light and y-linearly polarized light, as depicted in Figs. 1(a) and 1(b).

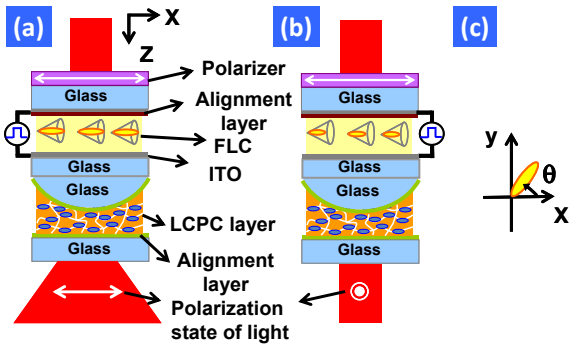

Fig. 1. Operating principles and the structure of the bistable negative lens at (a) e-state and (b) o-state. The white arrow of the polarizer indicates the transmissive axis. The propagation direction of incident light is along + z direction. (c) The top view of FLC directors of the FLC layer in (a) θ = 0, and θ = 46 degree means the LC lens is at e-state and at o-state, respectively.

When a positive pulse of sufficiently larger voltage is applied to the FLC layer, the FLC directors (the top view of the FLC layer in Fig. 1(c)) are aligned parallel to x-axis (i.e. θ = 0) [21–23]. Thus the x-linearly polarized light is unchanged after passing through the FLC layer and therefore experiences a negative lens power (P_{LC}) resulting from the summation of a positive lens power of the curved glass substrate and a negative lens power of the LCPC layer. P_{LC} then equals to $(n_g\text{-}n_e)/R$, where R is the radius of curvature of the curved glass substrate, n_e is extraordinary refractive index of LCPC layer, and n_g is refractive index of the curved glass substrate ($n_g < n_e$). As a result, the incident light is diverged after light passes through the whole structure which is operated as a negative lens, as depicted in Fig. 1(a). Figure 1(a) is defined as "e-state". Thereafter on applying the negative voltage pulse, with sufficiently large magnitude, to the FLC layer, the FLC directors (the top view of the FLC layer in Fig. 1(c)) switches to by cone angle i.e. 45 degree with respect to x-axis. The FLC layer thickness is set to meet the half-wave plate requirement where the phase retardation is: $2\pi/\lambda\times(n_{e,flc}-n_{o,flc})\times d=(2m+1)\times\pi$, where λ is wavelength, m is an integer, d is the thickness of the FLC layer, $n_{e,flc}$ is extraordinary refractive index of FLC, and $n_{o,flc}$ is ordinary refractive index of FLC. As a result, the x-linearly polarized light is converted to y-linearly polarized light by the FLC layer. For the y-linearly polarized light, P_{LC} then equals to $(n_g\text{-}n_o)/R$, where n_o is ordinary refractive index of LCPC layer. The y-linearly polarized light is still collimated because the refractive index of LCPC layer and that of the curved glass substrate are close to each other (i.e. $n_g \sim n_o$), as depicted in Fig. 1(b). Thus no focusing effect

#209037 - $15.00 USD Received 27 Mar 2014; revised 7 May 2014; accepted 16 May 2014; published 22 May 2014

exists in this condition and the state of the system is defined as “o-state”. Moreover, e-state and o-state are two bistable states because of intrinsic property of the FLC, with large spontaneous polarization and helix free configurations, to memorize different optical states [21–23]. The difference of the lens powers between the e-state and the o-state is $\Delta n/R$, where Δn is the birefringence of the LCPC layer (i.e. $\Delta n = n_e - n_o$). Therefore, a bistable negative lens by integrating a polarization switch of FLC with a passively anisotropic focusing element of the LCPC layer can be realized.

The fabrication of sample includes two parts: one is FLC layer fabrication and the other one is LCPC assembly. First for the FLC layer fabrication, we prepared two glass substrates coated with indium-tin-oxide (ITO) layers. One of them was coated with photo-alignment layer i.e. sulfonic azo dye SD1 (from Dai-Nippon Ink and Chemicals, Japan) and afterwards irradiated by a linearly polarized UV light (λ = 365 nm) to provide preferred direction of the easy axis for the FLC alignment, in the direction perpendicular to the plane of polarization of the irradiating light. Later on, the cell was assembled by these two substrates and the cell gap was maintained at 5 μm. A FLC (FLC-510, from Lebedev Physical Institute of Russian Academy of Sciences) was then filled into the cell at the temperature of 100°C and cooled slowly to room temperature [22]. The phase retardation was 3π radians and the cone angle (θ)was 46°. As for the LCPC part, we prepared a flat glass substrate and a plano-convex glass lens with a lens power of + 4.5 diopter (D) and a radius of curvature of 115mm. The flat glass substrate and a plano-convex glass lens were coated with mechanically buffered polyimide layers as alignment layers. The rubbing directions at the flat glass substrate and a plano-convex glass lens were anti-parallel. We then used the one drop filling (ODF) method to sandwich nematic LC (LCM1790, Δn = 0.41 for λ = 633nm at 21°C, LCMatter), reactive mesogen (RM257, Δn = 0.18 for λ = 633nm, Merck) and photoinitiator (IRG-184, Merck) at a ratio of 20:79:1 wt% between the flat glass substrate and the plano-convex glass lens. We exposed the UV light(λ = 365 nm) to the LCPC sample. After photo-polymerization, we attached the LCPC sample with the FLC sample together. The thickness in the center of LCPC layer was measured ~14.5 μm and the thickness in the peripheral was around 109 μm. Finally, we attached a polarizer outside the FLC sample in order to construct the structure in Fig. 1(a).

3. Experiment results and discussion

To demonstrate the concept, we first measured the electro-optic properties of the FLC sample only. A He-Ne laser used as a light source (λ = 632.8 nm) impinged on the FLC sample placed between two crossed polarizers. The FLC directors in e-state were parallel to the transmission axis of one polarizer. The opposite polarity voltage pulse with the pulse duration 10 msec was applied to the FLC cell. The time duration between adjacent pulses was 0.5 sec. The results are as shown in Figs. 2(a), 2(b), 2(c), and 2(d). In Figs. 2(a), 2(b), 2(c), and 2(d), the optical intensity increases with the amplitude of the pulsed voltage. The optical intensity reaches maximal and saturates as the amplitude of the pulsed voltage exceed 6V. This is because the polarization state of light is switched between x-linear polarization state and y-linear polarization state. In Fig. 2(c) or 2(d), the optical intensities in two different FLC switching positions, achieved on applying the voltage pulse of opposite polarity on FLC layer, are shown. It also indicates that the FLC sample exhibits not only bistability but also an ability of switching polarization of light, as the voltage is larger than 6V. The FLC sample, because of threshold, does not exhibits bistability for the voltage less than 4V. For the voltage in between 4V and 6V we observed the non-uniform and partially reoriented ferroelectric domain that results in the average optical intensity lower than the maximal [23]. In the following experiment, the amplitude of voltage pulse is set at 10 V because of a) the evident bistability with maximal transmission and b) fast response time.

To measure the phase profile and the lens power of the LCPC part, the LCPC sample was placed between two crossed polarizers and the rubbing direction was 45 degree with respect to one of the transmissive axis of polarizers. A He-Ne laser (λ = 633 nm) was used as a light source. Figure 3(a) shows the phase profile of the LCPC sample. The image exhibits

#209037 - $15.00 USD Received 27 Mar 2014; revised 7 May 2014; accepted 16 May 2014; published 22 May 2014

concentric circles due to the phase retardation of two orthogonally linear polarizations of lights [2]. The adjacent bright fringes in Fig. 3(a) represent optical phase difference of 2π radians. Optical phase difference equals $2\pi \times \Delta n \times d / \lambda$, where d is the optical path of LCPC sample. As a result, Fig. 3(a) can be converted to a spatial distribution of optical phase difference, as shown in Fig. 3(c). We also use a wavefront sensor (Thorlab, WFS-150-7AR) to measure the phase profile. A He-Ne laser (λ = 633 nm) was coupled to a fiber. The light came from the fiber was viewed as a point source. The light of the point source passed through a lens to generate a collimated light. The collimated light impinged on a polarizer, LCPC sample and two lenses which were used to adjust the beam size and the wavefront sensor, accordingly. The transmissive axis of the polarizer was parallel to the rubbing direction of LCPC sample. The measured phase profile of the LCPC sample using wavefront sensor is shown in Fig. 3(b). Furthermore, Fig. 3(a) and Fig. 3(b) are plotted as the optical phase difference vs. position. The phase profiles using two methods are similar. The lens power calculated from Fig. 3(c) is based on parabolic approximation of the optical phase difference. The lens power of the LCPC sample is −1.74 m^{-1} (diopter, D). When the transmissive axis of the polarizer is perpendicular to the rubbing direction of LCPC sample, the wavefront is flat which means no focusing effect (i.e. 0D).

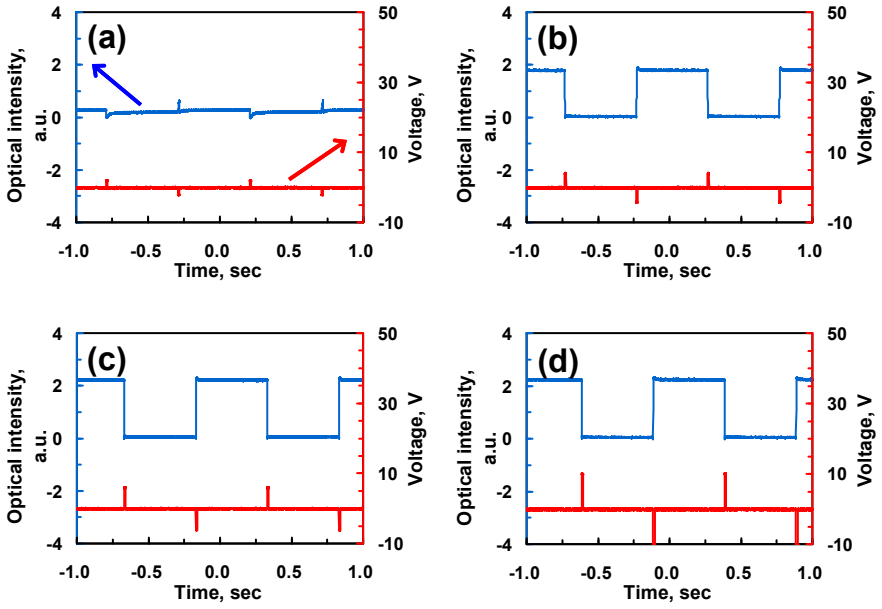

Fig. 2. Electro-optical properties of the FLC sample under pulsed voltages of (a) 2V, (b) 4V, (c) 6V, and (d) 10V.

#209037 - $15.00 USD Received 27 Mar 2014; revised 7 May 2014; accepted 16 May 2014; published 22 May 2014

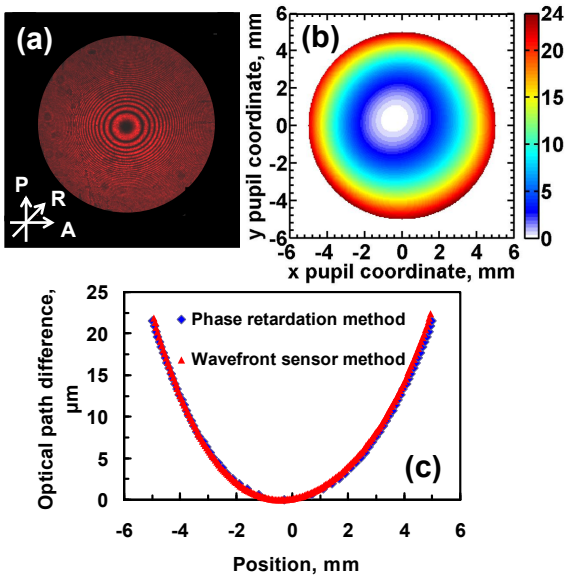

Fig. 3. (a) The image of the LCPC sample placed between two crossed polarizers. (b) The measured phase profile of the LCPC sample. The color bar indicates phase difference in the unit of micron. (c) The optical phase difference as a function of position.

Next, we assembled FLC sample to LCPC sample and then measured the phase profile using the wavefront sensor again. The result is shown in Fig. 4(a) and Fig. 4(b). Figures 4(a) and 4(b) are the phase profiles of the assembled sample at a pulsed voltage of + 10V (e-state) and at a pulsed voltage of −10V (o-state). From Fig. 4(a) and Fig. 4(b), it also confirmed that the assembled sample is a negative lens [Fig. 4(a)] and a lens without lensing effect [Fig. 4(b)]. On comparing Fig. 3(b) and Fig. 4(a), the phase profile in Fig. 4(a) of the assembled sample is distorted a little because of non-uniform thickness of the FLC sample resulting in non-uniform phase retardation. As a result, the output wavefront is distorted by not only x-linearly polarized light, but also elliptically polarized light. The optical responses of the assembled sample were recorded by a photodetector connected to an oscilloscope. The results are shown in Fig. 4(c). The incident light is diverged by the assembled sample when the voltage was switched from voltage-off state to e-state. The optical intensity is unchanged as the voltage is turned off. This shows bistability of the assemble sample. The response time is defined as the time difference between 10% and 90% of optical intensity. The response time in Fig. 4(c) is 0.171 ms. Thus, the assembled sample indeed exhibits not only bistability, but also fast response time.

#209037 - $15.00 USD Received 27 Mar 2014; revised 7 May 2014; accepted 16 May 2014; published 22 May 2014

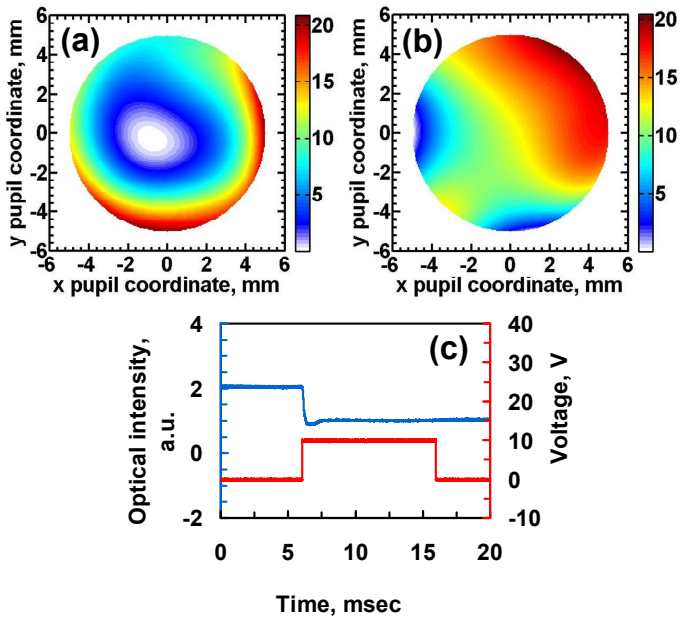

Fig. 4. The measured phase profile of the assembled sample at (a) e-state(+ 10V) and (b) o-state(−10V). (c) Optical intensity of the assembled sample as a function of time with applied voltages.

To test the image performance of the assembled sample, we placed two objective charts at 100cm and 37cm in front of the assembled sample attached with a polarizer. The light source is a white light source with an attached red color filter (λ = 600nm~700nm). The assembled sample was placed right in front of a camera. First the camera was adjusted, without the assembled sample, so that the corresponding image at the camera was observed clearly when the objective chart was at 37cm. Thereafter we attached the assembled sample with a polarizer back to the camera. The assembled sample was applied a pulsed voltage of −10V(o-state) and we adjusted the transmissive axis of the polarizer in order to observe the clear image for the object of 37cm, as shown in Fig. 5(a). Figure 5(b) is the image when the voltage was turned off after o-state. The image remains the same at o-state. Similarly, Fig. 5(c) is the image when the assembled sample was at e-state. The image remains the same at e-state after the voltage was turned off, as shown in Fig. 5(d). In Fig. 5, the objective chart at 37cm and at 100cm are clear at −10V and + 10V, respectively. This means the camera can see further with the assembled sample and also confirm that the assembled sample is an electrically switchable negative lens. In fact, in order to see the object clearly from 37cm to 100cm, the requirement of the lens power of the assemble sample should be (100/100) - (100/37) = −1.7 D, which is closed to the lens power of LCPC sample ~1.74D.

#209037 - $15.00 USD Received 27 Mar 2014; revised 7 May 2014; accepted 16 May 2014; published 22 May 2014

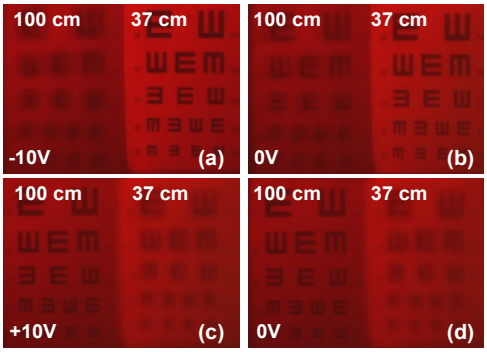

Fig. 5. Image performance of the assembled sample (a) at o-state (−10V). (b) After the voltage was turned off, the image remains the one at o-state. (c) Image performance at e-state (+ 10V). (d) After the voltage was turned off, the image remains the one at e-state.

In the experiments, we estimate the Δn of LCPC layer ~0.2 according to the change of the lens power (~1.74D) of the LCPC layer which equals Δn/R, where R = 115 mm. Theoretically, Δn of LCPC layer consisting of reactive mesogen (RM257) and liquid crystal (LCM1790) should be around 0.224 (i.e. $0.41\times0.2+0.18\times0.79=0.224$) closed to experiments. To further improve the change of the lens power, we can increase the concentration of liquid crystals of LCPC layer, replace the reactive mesogen with higher birefringence, or decrease the radius of curvature R. To enlarge the aperture size, we can also increase the thickness of the LCPC layer or adopting a lens configuration based on diffraction. The proposed bistable lens assembly is designed for red light that can be changed for different wavelength by changing the phase retardation of FLC and LCPC parts [24]. For broadband applications, we can replace the FLC sample with an achromatic phase retarder using zential bistable twist nematic switchs, optical rewritable twist nematic, or even adopting several FLC layers with phase retardation of π radians [24–26].

4. Conclusion

In conclusion, we demonstrate an electrically bistable negative lens by integrating a polarization switch of FLC with a passively anisotropic focusing element of a LCPC layer. The function of FLC layer serves as an electrically bistable polarization switch and thus affect the focusing properties of the passively anisotropic focusing element. The lens structure we proposed not only exhibits bistability but also fast response time of sub-ms. Small non-uniformity in the phase profile can be attributed to the non-uniform cell gap and imperfect FLC alignment. However, this can be improved by changing the anchoring energy of the alignment layer (i.e. SD1) by mean of different irradiation energy [27]. The tunable lens power is from −1.74D to 0D for the aperture size of 10mm. The lens power can be changed easily by changing the curvature of the glass substrate in LCPC part and the thickness of the LCPC layer. The aperture size can even be enlarged for the sunglasses with prescription. The impact of this study is to provide a solution of electrically bistable LC lenses for the applications of a switch in optical systems, shutters, sensors, portable devices, wearable devices and colored ophthalmic lenses.

Acknowledgments

This research was supported partially by the National Science Council (NSC) in Taiwan under the contract no. NSC 101-2112-M-009-011-MY3 and partially by Liqxtal Technology Inc. The HK Gov. grant no. ITP/039/12NP is also gratefully acknowledged

#209037 - $15.00 USD Received 27 Mar 2014; revised 7 May 2014; accepted 16 May 2014; published 22 May 2014